Hubble Space Telescope imaging survey of sub-mJy star-forming galaxies — I. Morphologies at *z* 0.2

Journal Item

Mon. Not. R. Astron. Soc. **317**, L29–L33 (2000)

Hubble Space Telescope imaging survey of sub-mJy star-forming galaxies – I. Morphologies at $z \sim 0.2$

Stephen Serjeant,[1★] Bahram Mobasher,[1,2†] Carlotta Gruppioni[1,3] and Seb Oliver[1,4]

[1]*Astrophysics Group, Blackett Laboratory, Imperial College, Prince Consort Road, London SW7 2BZ*
[2]*Space Telescope Science Institute, 3700 San Martin Drive, Baltimore, MD 21218, USA*
[3]*Osservatorio Astronomico di Bologna, via Ranzani 1, 40127 Bologna, Italy*
[4]*Astronomy Centre, CPES, University of Sussex, Falmer, Brighton BN1 9QJ*

Accepted 2000 June 1. Received 2000 May 18; in original form 2000 February 29

ABSTRACT

We present the first results of our *Hubble Space Telescope HST* WFPC2 F814W snapshot imaging survey, targeting virtually all sub-mJy decimetric radio-selected star-forming galaxies. The radio selection at ~1 GHz is free from extinction effects and the radio luminosities are largely unaffected by AGN contamination, making these galaxies ideal tracers of the cosmic star formation history. A subsample of four targets is presented here, selected at 1.4 GHz from the spectroscopically homogenous and complete samples of Benn et al. and Hopkins et al. The redshifts are confined to a narrow range around $z \sim 0.2$, to avoid differential evolution, with a radio luminosity close to L_* where the galaxies dominate the comoving volume-averaged star formation rate. We find clearly disturbed morphologies resembling those of ultraluminous infrared galaxies, indicating that galaxy interactions may be the dominant mechanism for triggering star formation at these epochs. The morphologies are also clearly different from those of coeval quasars and radio galaxies, as found in star-forming galaxies selected at other wavelengths. This may prove challenging for models that propose direct causal links between AGN evolution and the cosmic star formation history at these epochs. The asymmetries are typically much larger than seen in the Canada–France Redshift Survey at similar redshifts, optical luminosities and Hα-derived star formation rates, indicating the possible existence of an obscuration-related morphological bias in such samples.

Key words: surveys – galaxies: evolution – galaxies: formation – galaxies: starburst – cosmology: observations – infrared: galaxies.

1 INTRODUCTION

The study of the observational constraints on the cosmic star formation history is currently among the most active fields in observational cosmology. The most widely used tracer of the comoving volume-averaged star formation rate (SFR) is the UV luminosity density (e.g. Madau et al. 1996; Steidel et al. 1996, 1999), found to peak at $z \sim 1$–2. However, little is known about the history of star formation in the Universe beyond its global average (e.g. Abraham et al. 1999). In this paper we present the first results from an on-going programme with the *Hubble Space Telescope* (*HST*) to study the morphology of star-forming galaxies, using a sample of galaxies that dominate the comoving SFR and which were selected in a manner free from obscuration biases.

An important caveat to the SFR constraints is that the UV luminosity of star-forming galaxies is dominated by the lowest extinction regions. This leads to extreme sensitivity to obscuration corrections (e.g. Meurer et al. 1997; Pettini et al. 1998), large enough to eliminate the evidence for a redshift cut-off in the SFR. Indeed, observations with the Submillimetre Continuum Bolometer Array (SCUBA) of the *Hubble Deep Field* (HDF) (Hughes et al. 1998) detected five ultraluminous galaxies at $z > 2$ (the redshift constraints come mainly from the radio–far-infrared correlation and not from the uncertain HDF identifications), which together implied an obscured SFR at least as large as the integrated dereddened UV-derived rate. Moreover, the Hα-derived SFR from the Canada–France Redshift Survey (CFRS: Tresse & Maddox 1998) was a factor of ~3 larger than the UV estimate in the same sample, but comparable to those derived from the mid-infrared for the CFRS (Flores et al. 1999) or the HDF (Rowan-Robinson et al. 1997).

However, a serious problem is that optical–UV light is strongly

★ E-mail: s.serjeant@ic.ac.uk
† Affiliated with the Astrophysics Division, European Space Agency.

skewed to low-extinction regions, while the reverse is true for mid- and far-infrared-selected samples, leading to problematic obscuration-related effects in either case. An unbiased technique for selecting star-forming galaxies is to sample at decimetric radio wavelengths, where both obscured and unobscured star-forming galaxies contribute (Condon 1992). Several groups (including ourselves) have begun to exploit this technique to trace the comic star formation history, and to study the obscuration effects in star-forming galaxies (e.g. Cram et al. 1998; Serjeant, Gruppioni & Oliver 1998; Oliver, Gruppioni & Serjeant 1998; Haarsma & Partridge 1998; Cram 1998, etc.).

We have embarked on a programme to image almost all star-forming galaxies selected at decimetric radio wavelengths, using the Wide Field Planetary Camera 2 (WFPC2) in snapshot mode on the *HST*. In this paper we carry out a morphological study of a small subset of these galaxies at $z \sim 0.2$, from our first cycle 8 observations in this programme. [Although these are at low redshifts by many standards, they are *not* local, with the volume-averaged SFR being a factor of ~2 higher than in the local Universe for $(1+z)^3$ luminosity evolution models (Table 1).] The galaxies in this sample are selected so that they dominate the (radio-derived) star formation history of the Universe at this epoch, i.e. close to the L_* characteristic luminosity in the radio luminosity function.

The sample selection is discussed in Section 2, which also presents the *HST* observations and data reduction. These data are then analysed in Section 3, followed by a discussion of the results in Section 4.

Table 1. Flux of the break in the 1.4-GHz luminosity function (L_*) under various luminosity evolution assumptions. The table uses the luminosity function from Serjeant et al. (1998), with an $\Omega = 1$, $\Lambda = 0$ world model. Very similar results are derived from the Condon (1992) luminosity function. For a Hubble constant of $H_0 = 50\,\mathrm{km\,s^{-1}\,Mpc^{-1}}$, the characteristic luminosity lies at $\sim 2.8 \times 10^{22}$ $\mathrm{W\,Hz^{-1}}$. The fluxes themselves are H_0-independent.

Redshift	Evolution	L_* 1.4-GHz flux (mJy)
0.2	$(1+z)^3$	0.264
0.2	none	0.153
0.3	$(1+z)^3$	0.145
0.3	none	0.066

2 SAMPLE SELECTION AND OBSERVATIONS

The following criteria are considered in selecting the sample for *HST* observations.

(i) The objects are sub-mJy radio sources, selected at 1.4 GHz (Benn et al. 1993; Georgakakis et al. 2000). This avoids obscuration-related selection biases. Decimetric radio fluxes are much less affected by AGN contribution than shorter wavelength observations [e.g. the ongoing controversy over the AGN fraction in higher frequency samples, with Hammer et al. (1995) finding a ~50 per cent AGN fraction at 5–8 GHz while Windhorst et al. (1995) find only ~5 per cent].

(ii) Spectroscopic data are used to select emission-line star-forming galaxies.

(iii) The galaxies must not lie close to bright stars, to avoid *HST* roll angle constraints.

(iv) The galaxies must lie close to the 1.4-GHz L_*, which dominates the volume averaged SFR (Table 1).

(v) The galaxies must lie in a narrow redshift range around $z \sim 0.2$ to avoid differential evolution.

Our primary sample satisfies (i), (ii) and (iii), and is the subject of our 150 snapshots in cycles 8 and 9. Ten galaxies also satisfy conditions (iv) and (v); these are the cycle 8 targets. The *HST* observations for four of these have now been completed. We selected the F814W (wide *I* band) filter. At this wavelength, the light is mostly dominated by the old stellar population, so gives a more accurate measure of distortion in the underlying gravitational potential than e.g. UV observations. Details of the current subsample are presented in Table 2.

The data were reduced using the Interactive Data Language (IDL), starting from the automatic pipeline products. Cosmic rays were identified as $>3\sigma$ differences between frames. For sky subtraction, we estimated the modal value of the underlying counts distribution using iterative fits to the readout histograms. The final *HST* images for the four sub-mJy radio sources are presented in Fig. 1.

3 RESULTS

[CM84] 144 is extremely disturbed, with a tidal tail extending ~1.5 arcsec north-east of the nucleus. Several secondary nuclei are also apparent, reminiscent of *HST* WFPC2 F814W imaging of ultraluminous infrared galaxies (e.g. Borne et al. 2000) such as Arp 220 (Borne & Lucas, in preparation).

[CM84] 074 is only mildly asymmetric. There are hints of face-on spiral structure, and an excess flux ~0.5 arcsec west of the nucleus. There are two companion galaxies a few arcseconds to

Table 2. The *HST* $z \sim 0.2$ sub-mJy star-forming snapshot sample observed to date. All were observed for 2×400 s with the Planetary Camera in filter F814W. References are: (1) Georgakakis et al. (2000); (2) Condon & Mitchell (1984); (3) Rowan-Robinson et al. (1993); (4) Benn et al. (1993); (5) Hopkins et al. (1998); (6) Hopkins et al. (1999). SFRs (1.4 GHz and Hα) are in $\mathrm{M_\odot\,yr^{-1}}$, and A is the asymmetry. For comparison, the $z = 0.2$ ($z = 0.3$) radio L_* assuming $(1+z)^3$ luminosity evolution corresponds to $63.4\,\mathrm{M_\odot\,yr^{-1}}$ ($80.6\,\mathrm{M_\odot\,yr^{-1}}$). The Tresse & Maddox (1998) Hα L_* at $z \sim 0.2$ corresponds to $22.4\,\mathrm{M_\odot\,yr^{-1}}$.

Name	RA (J2000)	Dec. (J2000)	Mag	z	$S_{1.4}$ (mJy)	I_{814}	M_B (AB)	SFR (1.4)	SFR (Hα)	A
[CM84] 144[2,3,4]	08 55 47.60	+17 02 28.4	$B = 18.7$	0.2253	0.29	18.3	−21.2	116.3	12.9	0.47
[CM84] 074[2,3,4]	08 54 58.33	+17 03 46.9	$B = 18.6$	0.2279	0.29	18.7	−20.8	117.6	8.34	0.112
Phoenix-Deep-29[1,5,6]	01 10 43.88	−45 51 22.7	$R = 20.2$	0.210	0.198	19.7	−19.6	52.5	1.1	0.185
Phoenix-Deep-96[1,5,6]	01 12 25.21	−45 47 0.1	$R = 18.4$	0.236	0.225	18.3	−21.2	75.9	31.0	0.317

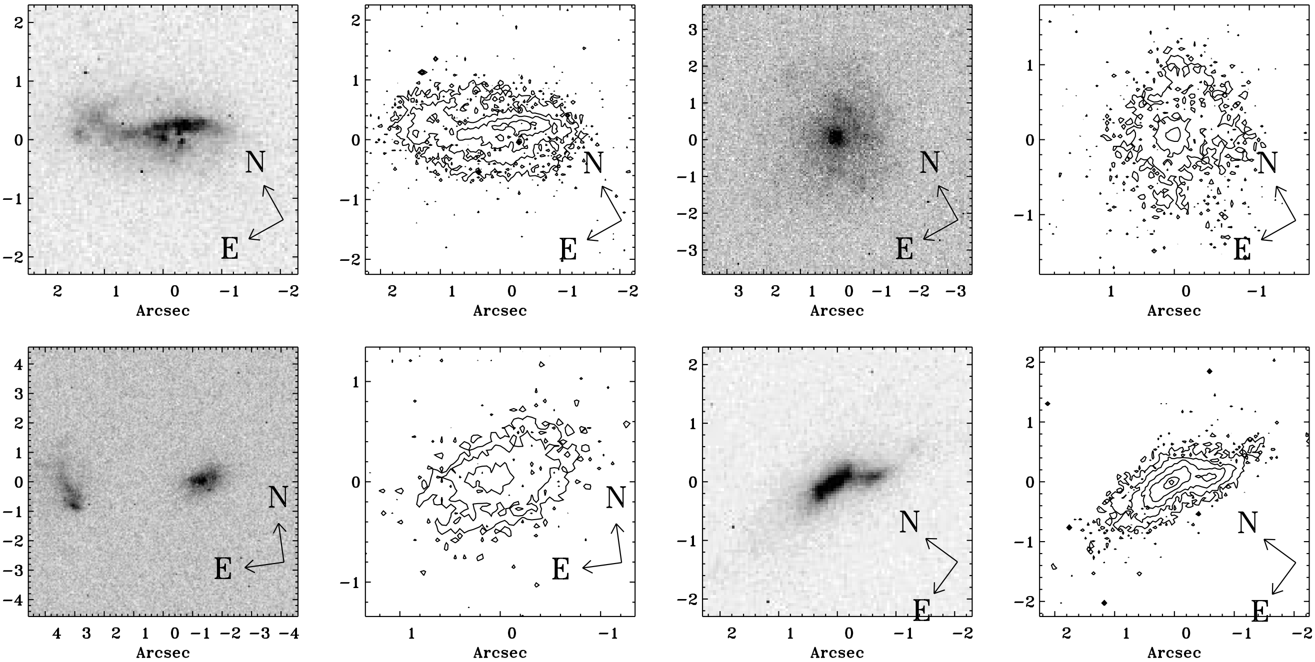

Figure 1. *HST* F814W snapshots of the galaxies [CM84] 144 (top left), [CM84] 074 (top right), Phoenix-Deep-29 (bottom left) and Phoenix-Deep-96 (bottom right). The grey-scale is linear, and contours are spaced in factors of 2.

the west, also visible in the Digitized Sky Survey. [We reject these as identifications of the radio source based on the ID magnitude quoted by Benn et al. (1993).]

Galaxy Phoenix-Deep-29 is again not as clearly disturbed. However, the inner isophotes are clearly offset in position and (tentatively) in orientation from the outer isophotes. This galaxy also shows signs of interaction with a companion 5 arcsec to the east. There is a clear tidal tail from the companion extending a few arcseconds north.

Galaxy Phoenix-Deep-96 shows clear signs of morphological disturbance, with the structure dominated by a bright central bar-like feature. There are also hints of multiple nuclei inside the bar, and there is a secondary peak ~0.5 arcsec south-west of the bar. There are, however, no other clearly associated companion galaxies visible in the *HST* image.

To quantify the morphological disturbance, we follow the procedure adopted by Brinchmann et al. (1998) and others, by rotating each image through π radians and subtracting it from the original image. Normalizing this to the galaxy flux yields the fractional asymmetric flux:

$$A = \frac{\sum |G_{ij} - G'_{ij}|}{\sum G_{ij}} - k, \qquad (1)$$

where G (G') is the rotated (unrotated) image, k is a correction for systematics such as sky gradients, and the sum is performed over pixels ij. The values of A are fairly insensitive to the choice of aperture used for the self-subtraction, provided that all pixels at $\gtrsim 1.5\sigma$ are included in the subimage. The magnitude of k can be estimated by applying the technique to blank sky regions of the same size. The errors in A are in practice dominated by the uncertainty in k: we find typically $\Delta A \simeq 0.05$. A further advantage of this statistic is that the I-selected CFRS and the b_J-selected Low Dispersion Survey Spectrograph (LDSS) have extensive published *HST* morphologies quantified using the same statistic, yielding valuable control samples. The asymmetry measures for the sub-mJy star-forming galaxies, quantified as discussed above, are listed in Table 2.

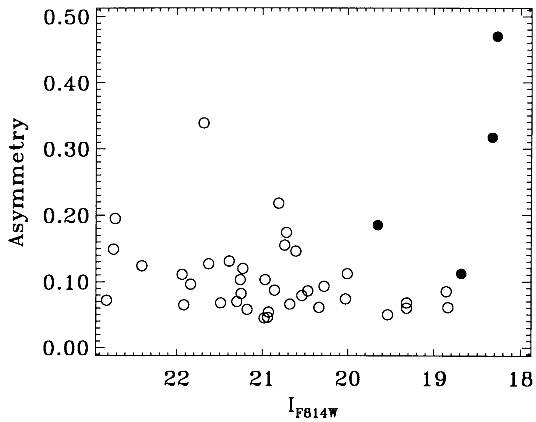

Figure 2. Asymmetry parameters for the radio-selected sub-mJy star-forming galaxies (filled symbols) compared with the CFRS/LDSS galaxies with $0.17 \leqslant z \leqslant 0.3$ (open symbols).

4 DISCUSSION AND CONCLUSIONS

In Fig. 2 we plot the asymmetry statistics of our galaxies, and compare them with a control sample of coeval galaxies from the CFRS sample (Brinchmann et al. 1998). The control extends to fainter I_{F814W} fluxes than our star-forming galaxy sample, though there is some overlap. Remarkably, our galaxies are far more asymmetric than the control sample of an (ostensibly) identical population of optically selected star-forming galaxies of the same I_{F814W}.

The optical control must be well-matched with the radio sample in as many *optical* properties as possible. The radio sample is

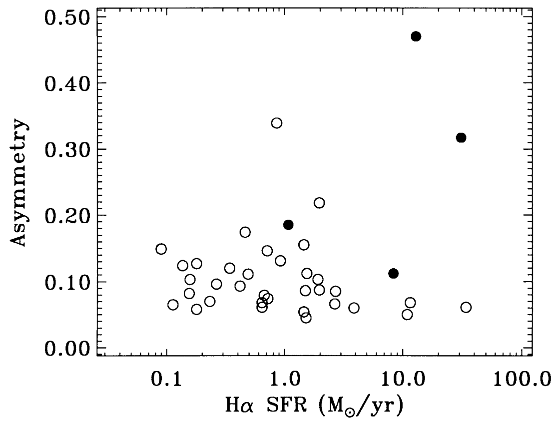

Figure 3. The asymmetry parameter plotted against the estimate of the Hα SFR discussed in the text. Symbols are as in Fig. 2.

more asymmetric at a fixed optical luminosity, but is this also true at a fixed optically derived SFR? In other words, could the morphological differences between the radio sample and the optically selected control be instead because they are not well-matched in optically derived SFRs? To address this we must compare the Hα luminosities of our radio sample with those of the control. The data for the radio samples are presented by Benn et al. (1993) and Georgakakis et al. (2000). The individual Hα luminosities of the CFRS galaxies are not published, but Tresse & Maddox (1998) report a tight correlation between Hα luminosities and $M_B(AB)$ absolute magnitudes. In Fig. 3 we use this relation to estimate the Hα-derived SFRs, and compare the optical control sample with our sub-mJy star-forming galaxies. We adopt the following conversion between Hα luminosities and SFRs (SFRs):

$$\mathrm{SFR(H\alpha)} = L(\mathrm{H\alpha})/(1.41\times10^{34}\,\mathrm{W}), \qquad (2)$$

which is derived assuming a Salpeter initial mass function (IMF) between 0.1 and 125 $\mathrm{M}_\odot$ (see Serjeant et al. 1998; Oliver et al. 1998). We de-redden our Hα fluxes by $A_V = 1$ for consistency with optically selected samples. [Tresse & Maddox (1998) noted that the Hα luminosity function is essentially unchanged if assuming this A_V throughout their sample, instead of using individual Balmer decrements.] There is a more substantial overlap of the Hα-derived SFR with the control sample, and it is again clear that at a *fixed* Hα SFR the radio-selected sample is significantly more disturbed than the optically selected sample of star-forming galaxies.

In summary, the radio-selected sources are typically more morphologically disturbed than the optically selected control, well-matched in redshift, optical luminosity and/or Hα SFR. Why this might be the case is hinted at in Table 2, where we compare the SFRs of our galaxies estimated from Hα and the 1.4-GHz radio luminosity. To convert decimetric radio luminosities to SFRs we use

$$\mathrm{SFR(1.4\,GHz)} = L_{1.4}/(7.63\times10^{20}\,\mathrm{W\,Hz^{-1}}), \qquad (3)$$

appropriate for the same IMF as above (see Oliver et al. 1998; Serjeant et al. 1998). Our Hα SFRs are comparable in most cases to $L*$ in the Hα luminosity function (Tresse & Maddox 1998). However, the radio-derived SFRs are much larger (although still comparable to the radio $L*$: Table 1). This indicates that a large fraction of the star formation in these objects occurs in regions with $A_V \gg 1$, since the observed Hα luminosities will be dominated by regions with $A_V \lesssim 1$. Indeed, if the dust is well-mixed with the Hα-emitting gas, the different optical depths for Hα and Hβ ensure that $A_V = 1.1$ would be derived for a simple screen Balmer decrement model *regardless* of the true extinction to the rear of the cloud. We therefore suggest that optically selected samples may under-represent disturbed galaxies with large amounts of obscured star formation, in any SFR-weighted quantity.

The galaxy morphologies of the sub-mJy sources are also markedly different from those of coeval AGN. McLure el al. (1999) and McLeod & Rieke (1995) have found giant ellipticals hosting both radio-loud and radio-quiet quasars at these redshifts, and radio galaxies are also early-type galaxies at these epochs. The Einstein Extended Medium Sensitivity Survey (EMSS)-selected sample of Schade, Boyle & Letawsky (1999) at $z \leqslant 0.15$ also finds no evidence for strong interaction/merger activity for any AGN in the sample. This may pose problems for models that propose causal links between the cosmic evolution of AGN and the cosmic star formation history. For example, a model in which both are driven by similar merger events must also provide a mechanism for delaying the onset of central engine fuelling, to account for the (relatively) more relaxed AGN host galaxy potentials. This is related to the more fundamental and unsolved problem of AGN evolution: how to drive the gas fuel down ~5 orders of magnitude in radius.

We can also compare our sample with the ultraluminous galaxy samples of e.g. Borne et al. (2000), who also used *HST* WFPC2 F814W in snapshot mode. These authors found highly disturbed systems often in moderately rich environments, which they used to argue for an evolutionary sequence involving compact groups and ultraluminous galaxies. Although asymmetry statistics have not been calculated for the ultraluminous galaxies, our targets appear qualitatively less disturbed and the environments possibly less rich. [Ideally both ultraluminous galaxies and radio-selected star-forming galaxies should also have their environments quantified with, for example, the B_{gg} statistic (e.g. Yee & Green 1984; Hill & Lilly 1991; Wold et al. 2000).] This may suggest a link between the level of star formation activity after interactions and the richness of the environment, perhaps via the number or the nature of the interaction events.

Although our current sample is small, the asymmetric morphologies in our ~$L*$ targets suggest that galaxy interactions play a major role in the evolution of the star formation and metal production rates in the low-z Universe. Further papers in this series will present results for larger samples of sub-mJy star-forming galaxies. However, it is worth keeping in mind that the formation and evolution of galaxies cannot be characterized by a single parameter, such as the volume-averaged SFR. In expanding on this simple first-order description, the obscuration-independent selection of galaxies will be essential, as will coordinated multi-wavelength follow-up [e.g. the European Large Area *ISO* Survey (ELAIS): Oliver et al. 2000].

ACKNOWLEDGMENTS

It is a pleasure to thank Patricia Royle for her help in the preparation of these observations. This paper is based on observations with the NASA/ESA *Hubble Space Telescope*, obtained at the Space Telescope Science Institute, which is operated by the Association of Universities for Research in Astronomy, Inc., under NASA contract No. NAS5-26555. This work was supported by PPARC (grant number GR/K98728) and by the EC TMR Network programme (FMRX-CT96-0068).

REFERENCES

Abraham R. G., Merrifield M. R., Ellis R. S., Tanvir N. R., Brinchmann J., 1999, MNRAS, 308, 569
Benn C. R., Rowan-Robinson M., McMahon R. G., Broadhurst T. J., Lawrence A., 1993, MNRAS, 263, 98
Borne K. D., Bushouse H., Lucas R. A., Colina L., 2000, ApJ, 529, L77
Brinchmann J. et al., 1998, ApJ, 499, 112
Condon J. J., 1992, ARA&A, 30, 575
Condon J. J., Mitchell J. J., 1984, AJ, 89, 610
Cram L., 1998, ApJ, 506, L85
Cram L., Hopkins A., Mobasher B., Rowan-Robinson M., 1998, ApJ, 507, 155
Flores H. et al., 1999, ApJ, 517, 148
Georgakakis A., Mobasher B., Cram L., Hopkins A., Lidman C., Rowan-Robinson M., 2000, MNRAS, 306, 708
Haarsma D. B., Partridge R. B., 1998, ApJ, 503, L5
Hammer F., Crampton D., Lilly S. J., Le Fèvre O., Kenet T., 1995, MNRAS, 276, 1085
Hill G. J., Lilly S. J., 1991, ApJ, 367, 1
Hopkins A. M., Mobasher B., Cram L., Rowan-Robinson M., 1998, MNRAS, 296, 839
Hopkins A., Afonso J., Cram L., Rowan-Robinson M., 1999, ApJ, 519, L59
Hughes D. et al., 1998, Nat, 394, 421
McLeod K. K., Rieke G. H., 1995, ApJ, 454, L77
McLure R. J., Kukula M. J., Dunlop J. S., Baum S. A., O'Dea C. P., Hughes D. H., 1999, MNRAS, 308, 377
Madau P., Ferguson H. C., Dickinson M. E., Giavalisco M., Steidel C. C., Fruchter A., 1996, MNRAS, 283, 1388
Meurer G. R., Heckman T. M., Lehnert M. D., Leitherer C., Lowenthal J., 1997, AJ, 114, 54
Oliver S., Gruppioni C., Serjeant S., 1998, preprint (astro-ph/9808260)
Oliver S. et al., 2000, MNRAS, 316, 749
Pettini M., Kellog M., Steidel C. C., Dickinson M., Adelberger K. L., Gaivalisco M., 1998, ApJ, 508, 539
Rowan-Robinson M., Benn C. R., Lawrence A., McMahon R. G., Broadhurst T. J., 1993, MNRAS, 263, 123
Rowan-Robinson M. et al., 1997, MNRAS, 289, 490
Schade D., Boyle B. J., Letawsky M., 1999, preprint (astro-ph/9912294)
Serjeant S., Gruppioni C., Oliver S., 1998, preprint (astro-ph/9808259)
Steidel C. C., Giavalisco M., Pettini M., Dickinson M., Adelberger K. L., 1996, ApJ, 462, L17
Steidel C. C., Adelberger K. L., Giavalisco M., Dickinson M., Pettini M., 1999, ApJ, 519, 1
Tresse L., Maddox S. J., 1998, ApJ, 495, 691
Windhorst R. A., Fomalont E. B., Kellermann K. I., Partridge R. B., Richards E., Franklin B. E., Pascarelle S. M., Griffiths R. E., 1995, Nat, 375, 471
Wold M., Lacy M., Lilje P. B., Serjeant S., 2000, MNRAS, 316, 267
Yee H.K. C., Green R. F., 1984, ApJ, 280, 79

This paper has been typeset from a TEX/LATEX file prepared by the author.